



HHS Public Access

Author manuscript

Adv Funct Mater. Author manuscript; available in PMC 2017 April 19.

Published in final edited form as:

Adv Funct Mater. 2016 April 19; 26(15): 2512–2522. doi:10.1002/adfm.201504879.

Noninvasive Transdermal Vaccination Using Hyaluronan Nanocarriers and Laser Adjuvant

Dr. Ki Su Kim,

Wellman Center for Photomedicine, Massachusetts General Hospital, 65 Landsdowne St., UP-5, Cambridge, Massachusetts 02139, USA

Department of Dermatology, Harvard Medical School, 40 Blossom St., Boston, Massachusetts 02140, USA

Dr. Hyemin Kim,

Department of Materials Science and Engineering, Pohang University of Science and Technology (POSTECH), 77 Cheongam-Ro, Nam-gu, Pohang, Gyeongbuk 790-784, Korea

Dr. Yunji Park,

Division of Integrative Biosciences and Biotechnology, POSTECH, 77 Cheongam-Ro, Nam-gu, Pohang, Gyeongbuk 790-784, Korea

Dr. Won Ho Kong,

Department of Materials Science and Engineering, Pohang University of Science and Technology (POSTECH), 77 Cheongam-Ro, Nam-gu, Pohang, Gyeongbuk 790-784, Korea

Seung Woo Lee [Prof.],

Division of Integrative Biosciences and Biotechnology, POSTECH, 77 Cheongam-Ro, Nam-gu, Pohang, Gyeongbuk 790-784, Korea

Department of Life Science, POSTECH, 77 Cheongam-Ro, Nam-gu, Pohang, Gyeongbuk 790-784, Korea

Sheldon J. J. Kwok,

Wellman Center for Photomedicine, Massachusetts General Hospital, 65 Landsdowne St., UP-5, Cambridge, Massachusetts 02139, USA

Department of Dermatology, Harvard Medical School, 40 Blossom St., Boston, Massachusetts 02140, USA

Sei Kwang Hahn [Prof.], and

Wellman Center for Photomedicine, Massachusetts General Hospital, 65 Landsdowne St., UP-5, Cambridge, Massachusetts 02139, USA

Department of Dermatology, Harvard Medical School, 40 Blossom St., Boston, Massachusetts 02140, USA

Correspondence to: Sei Kwang Hahn, skhanb@postech.edu; Seok Hyun Yun, syun@hms.harvard.edu.
K.S.K. and H.K. contributed equally to this work.

Supporting Information

Supporting Information is available from the Wiley Online Library or from the author.

Department of Materials Science and Engineering, Pohang University of Science and Technology (POSTECH), 77 Cheongam-Ro, Nam-gu, Pohang, Gyeongbuk 790-784, Korea

Seok Hyun Yun [Prof.]

Wellman Center for Photomedicine, Massachusetts General Hospital, 65 Landsdowne St., UP-5, Cambridge, Massachusetts 02139, USA

Department of Dermatology, Harvard Medical School, 40 Blossom St., Boston, Massachusetts 02140, USA

Sei Kwang Hahn: skhanb@postech.edu; Seok Hyun Yun: syun@hms.harvard.edu

Abstract

Vaccines are commonly administered by injection using needles. Although transdermal microneedles are less-invasive promising alternatives, needle-free topical vaccination without involving physical damage to the natural skin barrier is still sought after as it can further reduce needle-induced anxiety and simplify administration. However, this long-standing goal has been elusive since the intact skin is impermeable to most macromolecules. Here, we show an efficient, non-invasive transdermal vaccination in mice by employing two key innovations: first, the use of hyaluronan (HA) as vaccine carriers and, second, non-ablative laser adjuvants. Conjugates of a model vaccine ovalbumin (OVA) and HA—HA-OVA conjugates—induced more effective maturation of dendritic cells *in vitro*, compared to OVA or HA alone, through synergistic HA receptor-mediated effects. Following topical administration in the back skin, HA-OVA conjugates penetrated into the epidermis and dermis in murine and porcine skins up to 30% of the total applied quantity, as revealed by intravital microscopy and quantitative fluorescence assay. Topical administration of HA-OVA conjugates significantly elevated both anti-OVA IgG antibody levels in serum and IgA antibody levels in bronchioalveolar lavage, with peak levels at 4 weeks, while OVA alone had a negligible effect. An OVA challenge at week 8 elicited strong immune-recall humoral responses. With pre-treatment of the skin using non-ablative fractional laser beams (1410 nm wavelength, 10 ms pulse duration, 0.2 mJ/pulse) as laser adjuvant, strong immunization was achieved with much reduced doses of HA-OVA (1 mg/kg OVA). Our results demonstrate the potential of the non-invasive patch-type transdermal vaccination platform.

Keywords

Hyaluronan; Vaccine; Transdermal delivery; Laser adjuvant; Transdermal Immunization; Non-invasive; Immunization

1. Introduction

Vaccines provide effective prevention and treatment of many infectious diseases.^[1] Presently, the most common method of vaccine administration is by injection using needles and syringes. However, needle-based immunization has several disadvantages. Needle injection is painful, causes needle phobia, leaves dangerous medical waste, and poses the risk of disease transmission by needle re-use. A variety of vaccine delivery systems in various different delivery routes have been investigated to make vaccination safer, simpler, less expensive, and more effective.^[2] However, the major challenge in transdermal vaccine

delivery comes from intrinsic skin barriers that prevent macromolecules, such as protein-based vaccines, from entering the body. Several methods to break the skin barrier have been suggested, including intradermal needles,^[3] powderjet,^[4] ultrasound,^[5] electrical pulses,^[6] and photothermal gold nanoparticles.^[7] However, these approaches suffered from invasiveness, low bioavailability, or need for special apparatus. Other non-destructive methods based on transdermal administrations (topical applications), such as cationic liposomes,^[8] polymeric nanoparticles,^[9] and synthetic protamine^[10] have been proposed for high skin penetration, but their standalone effectiveness thus far have been unsatisfactory unless adjuvants, such as immunogenic minerals and emulsions,^[11] Toll-like receptor ligands,^[12] viral vectors,^[9] or toxins,^[10, 13] are used simultaneously. Unfortunately, many of the currently employed adjuvants cause potentially harmful adverse effects, such as pain and swelling by local inflammation, or fever and immunotoxicity by systemic reaction.^[14] Recently, microneedle arrays that contain vaccines and adjuvants in lyophilized forms coated on or embedded in biodegradable polymer matrices have shown enhanced immunization and reduced pain compared to conventional intradermal needles.^[15, 16] Although promising, microneedles, typically one 600–1000 μm in length, still induce physical disruption of the skin barrier and, therefore, can cause discomfort and require sanitary procedures to prevent infection through the holes in the skin.

The skin is one of the preferred sites for vaccine delivery because of accessibility and the abundance of antigen presenting cells (APC), such as Langerhans cells in the epidermis and dermal dendritic cells (DCs).^[17] To boost immune response, several types of adjuvant have been used through inducing damage-associated molecular patterns. Recently, there have been various successful preclinical and clinical trials using laser beams to maximize immune responses, a technique called laser adjuvant.^[18–22] There are two regimes: ablative and non-ablative. Irradiation with high-energy ablative fractional laser beams boosts the immune response by enhancing the activation and motility of APCs^[18] and, also, enables vaccine to be delivered through the perforated skin structure.^[19] Non-ablative fractional laser adjuvant^[21, 22] uses much lower energy laser beams focused to the dermis to generate the microthermal activation of APCs, without causing any damage to the stratum corneum and epidermis. While this technique on its own is effectively noninvasive, in practice, additional physically disruptive methods are required to overcome the intact skin barrier, such as microneedle arrays^[21] or intradermal injection,^[22] to deliver vaccine deep into the skin.

Hyaluronan (HA), a natural macromolecule with intrinsically high permeability into the skin,^[23] has been investigated for use as a carrier for transdermal drug delivery. HA is a linear polysaccharide abundant in the extracellular matrix in the skin and is widely used as dermal fillers in dermatologic clinics. HA is one of the most hydrophilic molecules in nature but also has a lipophilic patch domain. The amphiphilic nature enables HA to diffuse through the stratum corneum. HA receptors are highly expressed in skin cells, such as keratinocytes in epidermis and fibroblasts in dermis,^[24] which facilitates gradient-enhanced diffusion.^[25] The efficient skin penetration of HA has been extensively reported.^[23–27] Current understanding is that several factors, such as skin hydration, HA receptor mediated transport, and specific structure of HA, contribute to the transdermal delivery of HA.^[23, 27] Recently, it is reported that HA can induce the structural change of keratin and the disorder of lipid organization in stratum corneum.^[26] While the exact mechanisms remains fully

understood, HA has been widely investigated as a delivery agent of small molecular drugs and micro-sized particles for intranasal delivery of influenza vaccines.^[28] Recently, we have shown that HA can serve as a transdermal nano-carrier of macromolecules, such as human growth hormone (hGH)^[27] and nano graphene oxide,^[29] as well as chemical drugs and peptides. In the tissue, HA is degraded to small fragments in the skin, releasing the drugs. The fragments are recognized in the body as damage associated molecular pattern (DAMP) molecules,^[30, 31] which can enhance immune response against antigens.

Here, we demonstrate the capability of HA as an efficient transdermal nano-carrier for noninvasive transdermal vaccination using HA-ovalbumin (OVA) conjugates as a model vaccine. By two-photon microscopy and quantitative fluorescence analysis, we show the efficient penetration of HA-OVA conjugate into murine and porcine skins. We find that HA-OVA conjugates activate naive DCs *in vitro* much more efficiently than OVA alone and a mixture of HA and OVA. We also find that HA-OVA conjugates induce higher immune response than OVA alone and a mixture of HA and OVA after intramuscular injection, reflecting the adjuvant-like role of HA in the vaccine conjugate. Topical administration of HA-OVA conjugates onto intact murine skins efficiently induces the production of OVA-specific antibodies, in both first and secondary immune responses, which establishes the practical potential of this novel approach for needle-free vaccination. Finally, using laser adjuvant, we can reduce the HA-OVA conjugate dosage required for transdermal vaccination to similar levels used for intramuscular administration, while also eliciting strong mucosal immunity.

2. Results

Vaccination with OVA alone elicits minimal immune response

We first tested transdermal immunization *in vivo* by OVA alone. Various doses of OVA (20, 200 and 500 μg) were applied to the back skin of mice (BALB/c, $n = 4$ each). After 4 weeks, the production of humoral (IgG) and mucosal (IgA) OVA-specific antibody in the blood serum was measured to be negligible at all doses up to 500 μg (Figure 1a). To boost immunization efficiency, the skin site was illuminated with non-ablative laser beams from a battery-powered hand-held laser prior to the topical application of OVA solution. The laser output consists of a total fifty-four 10-ms-long pulsed beams, each with energy of 0.2 mJ, in a 6-by-9 array pattern over an area of 9 mm by 13 mm. The histological analysis showed no discernible damage in the epidermis and stratum corneum, which is consistent with previous studies.^[22, 32] Even with pre-treatment of laser adjuvant, topical applications of OVA alone failed to induce a significant increase of antibody titers. This finding suggests that OVA alone cannot penetrate the skin barrier to induce immune response with or without laser adjuvants. It also indicates the intact skin barrier function after laser adjuvant.

Next, we tested intramuscular injection of native OVA alone. It has been reported that single intramuscular injection of OVA elicits limited antibody production, particularly without adjuvants.^[33, 34] In agreement with these results, we found that while IgG antibody production was higher than transdermal delivery at the same doses, the overall response was minimal and not significantly different from baseline at doses less than 500 μg (Figure 1b). The injection of a dose of 500 μg resulted in a moderately elevated IgG level at week 4, but

failed to establish recall immunity against an OVA challenge (50 μ g) test. This result indicates that the immunogenicity of OVA alone in the body is insufficient to stimulate efficient vaccination.

Synthesis of HA-OVA conjugates

We synthesized HA-OVA conjugates using site-specific coupling reaction (Figure S1 and Figure 2a). Aldehyde (ALD) groups were introduced to HA molecules (215 kDa) by treatment with sodium periodate. The resulting HA-ALD was conjugated to the N-terminal primary amines of OVA at a low pH around 5 by using the pKa difference between N-terminal primary amines and amines of lysine in OVA.^[35] The retention time of HA-OVA conjugate in gel permeation chromatography (GPC) decreased after conjugation (Figure 2b), whereas the GPC peak unchanged for a simple mixture of OVA and HA-ALD (data are not shown). From the peak area of unreacted OVA before purification, the conjugation efficiency was calculated to be about 80%. The number of OVA per HA chain ranged from 3 to 6. The circular dichroism (CD) spectrum of OVA has a mixed secondary structure of α -helix and β -sheet,^[36] and HA has a strong negative band at 210 nm.^[37] The CD spectrum of HA-OVA conjugates matched well with that of the mixture of HA-ALD and unconjugated OVA (Figure 2c), which indicates that the secondary structure of OVA was maintained after conjugation. The peak of the fluorescence emission spectra of OVA and HA-OVA appeared at 355 nm, which corresponds to tryptophan (Trp) residues, indicating that the polarity of the microenvironment of Trp residues was not changed after conjugation (Figure 2d). The reduced fluorescence intensity of HA-OVA conjugates was likely due to quenching by interaction of OVA tryptophan residues with HA. Quenching of intrinsic protein fluorescence ascribed to interaction with several kinds of polymers has been reported elsewhere.^[34] The immunological bioactivity of HA-OVA conjugates characterized by anti-OVA antibody in ELISA and Bradford assay was comparable to native OVA without conjugation (Figure 2e). HA-OVA conjugates exhibited excellent serum stability over 100 h, better than OVA (Figure 2f).

Cellular uptake of HA-OVA *in vitro*

To investigate cellular interaction of HA-OVA conjugates, we quantified the uptake of RhoB-labeled OVA, HA, and HA-OVA conjugates by murine JAWS II dendritic cell line and human epidermal keratinocytes *in vitro*. Keratinocytes express HA receptors and contribute to antigen recognition by secreting immune mediators and transferring antigens to local DCs.^[10, 38] HA-OVA-RhoB and HA-RhoB conjugates entered these HA receptor-expressing cells much more efficiently than OVA-RhoB (Figure S2a). When HA receptors, such as CD44, were blocked by pre-incubation of DCs and keratinocytes with an excessive amount of free HA, the cellular uptake of HA-OVA-RhoB conjugate was significantly reduced (Figure S2b), which suggests that the endocytosis of HA-OVA conjugates is primarily mediated by HA receptors on the cell surface.^[39] As the DCs matured, the number of MHC Class II molecules on the cell surface increased.^[40] HA-OVA conjugates induced 2.5-fold more maturation than OVA or HA alone 2 days after treatment (Figure 2g). The higher maturation efficiency suggests a role of HA in HA-OVA via HA receptor-mediated endocytosis. To characterize the response of immature DCs upon the uptake of HA-OVA conjugates, we imaged JAWS II cells for 2 days *in vitro*. Upon activation, the concentration

of major histocompatibility complex (MHC) class II in the cytoplasm increased considerably in the activated state (Figure 2h). We also measured the levels of various pleiotropic cytokines, such as IL-1, IL-6, TNF- α , and GM-CSF, which are associated with the elevated expression of MHC class II molecules. HA-OVA conjugates significantly enhanced cytokine release from matured DCs, more than HA or OVA alone (Figure 2i).

Intramuscular immunization with HA-OVA *in vivo*

We compared the effectiveness of HA-OVA with a mixture of OVA and HA in conventional intramuscular humoral immunization in mice (BALB/c). We found that anti-OVA IgG antibody titer in serum increased by 20 fold at 4 weeks after intramuscular injection of HA-OVA conjugate containing 20 μ g of OVA, compared to normal levels in sham treated (PBS injected) animals (Figure 3). At higher doses of HA-OVA (200 μ g or 500 μ g of OVA), the serum IgG concentration only marginally increased further, indicating saturation of the antibody production. A simple mixture of OVA and free HA (16 or 215 kDa) failed to elicit IgG production. Similarly, in another study, trimethyl chitosan (TMC)–OVA conjugates have been shown to induce higher immune responses than the mixture of TMC and OVA.^[34] These results confirm the synergistic adjuvant-like effect of HA in enhancing immunization efficiency.^[34, 41]

Transdermal penetration of HA-OVA in murine skins *in vivo*

To investigate the efficiency and dynamics of transdermal penetration, we topically applied rhodamine B (RhoB) conjugated OVA, HA, and HA-OVA, respectively, to mice (C57BL/6) at the back skin after carefully removing the hair by using an animal clipper.^[42] Intravital two-photon microscopy showed time-dependent increase of HA-OVA-RhoB conjugate (red) in the dermis (Figure 4a). By contrast, the vast majority of OVA-RhoB did not penetrate the skin and remained in the stratum corneum (Figure 4b). Depth-resolved quantification of RhoB fluorescence intensity showed efficient penetration of HA-OVA-RhoB conjugate in stark contrast to the limited penetration of OVA-RhoB. The depth profile exhibited noticeable spatial heterogeneity, indicating there might be preferred routes for transdermal delivery. Examining hair follicles in the skin, we did not observe any apparent sign of penetration of HA-OVA-RhoB conjugate through the skin layer surrounding the hair follicles, contrary to the previous hypothesis of inter-follicular delivery.^[43] Unexpectedly, time-lapse images suggested that the initial primary delivery route is associated with natural wrinkles. The penetrated HA-OVA-RhoB conjugates through wrinkles diffuse rapidly throughout the dermis (Figure 4c). Interestingly, HA-OVA-RhoB conjugate was hardly detected in the epidermis within 2 h after topical application (Figure 4c).

Confocal images of tissue sections harvested at 4 h after topical administration showed significant penetration of HA-OVA-RhoB and HA-RhoB conjugates into both epidermis and dermis, whereas OVA-RhoB remained largely in the stratum corneum (Figure 4d). The images showed that, following the initial penetration through the wrinkles, HA-OVA conjugates (50 μ g OVA) diffused directly from the stratum corneum to epidermis after a few hours of topical administration. At 4 h, the remaining solution outside the skin was collected, and we measured that 78% of the total applied OVA, 50% of HA, and 51% of HA-OVA, respectively, remained in the solution. Assuming that the rest of agents had penetrated

in the tissues and analyzing the spatial distribution of RhoB fluorescence, we determined that 21% of the total OVA-RhoB was present in the stratum corneum, 0.9% in the epidermis, and 0.1% in the dermis (Figure 4e). On the other hand, 33%, 13%, and 4% of HA-RhoB, and 30%, 11% and 8% of HA-OVA-RhoB conjugate were distributed in the stratum corneum, epidermis, and dermis, respectively (Figure 4e). Of the total 49% HA-OVA conjugates that were absorbed in the skin, about 39% (=19/49) of them were delivered to the epidermis and dermis in 4 h.

To visualize the interaction of HA-OVA conjugates with DCs *in vivo*, we imaged MHC class II-enhanced green fluorescence protein (eGFP) transgenic mice 2–4 h after topical administration. Depth-resolved two-photon microscopy images showed the accumulation of HA-OVA-RhoB conjugates at the surface and in the cytoplasm of dermal DCs (Figure 4f). The result suggests that the maturation and activation of DCs upon interaction with HA-OVA conjugates occur *in vivo*.

Migration of activated DCs to draining LNs

Following antigen recognition in the skin, the activated DCs migrate from the antigen entry site to a draining lymph node (LN) where the antigens are presented to the naive T cells in the LN to initiate adaptive immune responses.^[44] To confirm this essential step in immunization, cervical LNs, which are draining LNs of the back skin, were harvested at 2 days after topical administration. Fluorescence images of tissue sections of the LNs showed a large number of HA-OVA-RhoB conjugates, but almost no OVA-RhoB and HA-RhoB conjugates were detected in the LNs (Figure 5a). Considering the significant penetration (17%) of HA beyond the stratum corneum, the absence of HA in the LNs suggests that the transportation of HA-OVA conjugate to the LNs is predominantly cell-mediated rather than passive diffusion. To corroborate our imaging analyses, we treated fluorescein isothiocyanate (FITC)-labelled HA-OVA conjugates (HA-OVA-FITC) at the abdominal flank skin and performed flow cytometry of the cells in the draining inguinal and non-draining cervical LNs collected at 2, 4, and 6 days (Figure 5b). The number of CD11c+, MHC class II+ DCs that are associated with HA-OVA-FITC conjugate (high FITC fluorescence) was as much as 7% (+/- 3%) at day 2 in the draining LNs, much higher than ~2% in the non-draining LNs, which decreased over time at days 4 and 6 (Figure 5c). We further investigated whether migratory DCs carrying HA-OVA-FITC conjugate was indeed originated in skin. The majority of FITC-high DCs was devoid of CD8 commonly expressed in LN-resident DCs (Figure 5d). No apparent correlation was found between CD103 (aE integrin)+ DCs^[45] and HA-OVA-FITC conjugate. Taken together, the histology and cytometry data support that skin-resident DCs uptake HA-OVA conjugates, much more efficiently than free OVA or HA, and subsequently migrated to draining LNs.

Transdermal immunization without laser adjuvants

We tested the effectiveness of transdermal immunization in mice (BALB/c). HA-OVA conjugates with different amounts (20, 200 and 500 µg) of OVA were applied to the back skin of mice (n = 4 each). HA-OVA conjugates containing 20 µg of OVA showed minimal humoral responses. However, at higher doses of HA-OVA conjugate, significant anti-OVA IgG antibody titers were measured (Figure 6a).

Time-lapse titration measurement showed that the amount of anti-OVA IgG in the HA-OVA conjugate treated group peaked about 4 weeks after transdermal administration and decreased to a much lower non-immunized (baseline) level at week 8 (Figure 6b). Having confirmed this duration, we tested immunologic memory in the mice that were vaccinated with various methods (n = 4 each), including transdermal administration of OVA and HA-OVA conjugate (500 µg of OVA). Eight weeks after vaccination, when the first immune response had disappeared, 50 µg of OVA was intramuscularly injected to each mouse, and the blood concentration of OVA specific antibody was measured 4 days after the immune challenge. Mice vaccinated by transdermal administration of HA-OVA conjugate with 500 µg of OVA showed a strong recall immune response, whereas all the other groups did not show significant antibody production (Figure 6b). The second immune response in the vaccinated group was considerably stronger than the first immune response, particularly in the early stages since the anti-OVA antibody concentration at 4 days post challenge was as high as the maximum level achieved 4 weeks after initial topical administration (Figure 6b).

Transdermal immunization by HA-OVA with laser adjuvants

The minimum OVA dose in HA-OVA required to induce strong immune responses via the intact skin was 500 µg (25 mg/kg), 25 times more than the dose of 20 µg (1 mg/kg) for intramuscular needle-based immunization (Figure 3). Considering the significant delivery efficiency of HA-OVA across the skin barrier (19% after 4 hours in the epidermis and dermis, Figure 4f), we hypothesized that the large difference in the dose was in part due to the absence of needle-induced adjuvant effects in topical administration. HA-OVA solution was topically applied on back skin of BALB/c mice shortly after the illumination of laser adjuvant pulses (32 J total). Anti-OVA IgG titration in the serum obtained at 4 weeks after the immunization was significantly elevated from the control physiological level with an OVA dose of 20 µg (Figure 7). The IgG concentration at a dose of 50 µg was similar to those obtained with an intramuscular injection dose of 20 µg and transdermal dose of 500 µg without laser adjuvants. Anti-OVA IgA levels also showed a significant increase at a dose of 20 µg and further increased with the administered OVA amount in HA-OVA (Figure 7). Intramuscular immunization did not increase the IgA level, which is indicative of mucosal immunity.

Transdermal penetration of HA-OVA in thick porcine skins

We also investigated the penetration efficiency of HA-OVA conjugates in porcine neck skins, which have a similar thickness and hair density to the human skin.^[15] Two-photon microscopy images of the tissue sections obtained 6 h after a topical administration showed a marked penetration of HA-OVA conjugates into the epidermis and dermis (Figure 8a). Quantitative fluorescence analysis after anatomy-based image segmentation indicated that 60% of HA-OVA-RhoB was in the stratum corneum, 32% in epidermis, and 8% in dermis, whereas 95% of OVA-RhoB was confined in the stratum corneum (Figure 8b). Consistent with murine skins, we found indications of initial penetration of HA-OVA through wrinkles (Figure 8c). The enhanced penetration is attributed to the thinner epidermis around the wrinkles, which leads to short diffusion time across and high local concentration of HA-OVA conjugates in wrinkles; however, the possibility of higher permeability of the epithelia-cell junction near wrinkles should not be ruled out.^[46] HA-OVA conjugates accumulated in

the dermis around wrinkles at 2 h (Figure 8d) but are expected to distribute more uniformly throughout the skin over time.

3. Discussion

Our results demonstrate the feasibility of a noninvasive, laser-assisted HA-based transdermal vaccination platform (Figure 9). When topically applied to intact skin by using a simple patch, more than 19% of HA-OVA conjugates penetrate to the epidermis and dermis in 4 hours, and considerably more is likely delivered in 48 hours. Laser adjuvant reduced the minimum dose of OVA from 25 to 1 mg/kg. In terms of the dose efficiency, the non-invasive transdermal platform is comparable to intramuscular injection of HA-OVA (1 mg/kg). Importantly, the dose efficiency is higher than conventional intramuscular injection of OVA alone. Furthermore, the transdermal immunization induced both systemic (IgG) and mucosal (IgA) immune responses whereas intramuscular injection does not elicit the mucosal immune response.^[10]

In addition to the role as nano-carriers for vaccines, HA provides additional benefit through an adjuvant-like effect, by promoting the presentation of the antigen to Langerhans and dermal DCs.^[47] Despite the poor *in vivo* immunogenicity of OVA alone, conjugation of HA significantly enhanced vaccination efficiency. For intramuscular immunization, in which tissue penetration is not a factor, HA-OVA induced significantly higher immune response than OVA only and a simple mixture of OVA and HA. This result can be explained by the well-known role of HA as DAMP. Intrinsic HAs present in the healthy skin are polymers with high molecular weight (>1 MDa). At sites of inflammation, HA polymers are cleaved to smaller fragments, which are potent activators of DCs.^[48] The HA repeating unit of N-acetyl-D-glucosamine can promote the maturation and activation of DCs in skin and stimulate T cells.^[30, 47] In addition, it has been shown that DCs are activated by HA via toll-like receptor 4.^[44]

While the present work has been focused on testing the proof-of-concept, the remarkable efficiency motivates in-depth studies of physiological and immunological responses and safety of the approach. Furthermore, it would warrant investigations for testing the practical potential of HA-conjugated vaccine patches. We found that HA-OVA conjugates were stable after freeze-drying at $-20\text{ }^{\circ}\text{C}$. Various HA-conjugated vaccines may be distributed and stored in lyophilized powder forms, which can be readily dissolved in aqueous phase. The product can be easily sterilized using filter sterilization method same as other peptide or protein drugs.^[49] The synthesis process does not require any specific reactors or complex purification steps, so scale-up manufacture can be easily set up. The dissolved HA-vaccine can be easily applied to the skin in the forms of skin toners and lotions. In addition, HA-vaccine conjugates can be prepared in a solution state for formulation due to the stable amide bond formation between HA and vaccine, which can be easily incorporated into skin vaccine patches.^[9, 50] Unlike conventional intramuscular and intranasal vaccination methods, non-invasive skin patches would not require highly trained personnel for administration and thus may enable simple administration at home. Studies have shown that about 93% of children experience serious immunization-related stress due to needle phobia^[51], and more than 10% of adults in the United States have needle fear^[52]. Needle-

free skin patches may encourage more people to take vaccination, ultimately reducing the healthcare costs. The combination of laser adjuvant and HA-vaccine patches may prove to be an attractive alternative to traditional intramuscular injection or emerging transdermal microneedle arrays.

4. Experimental Section

Synthesis and labelling of HA-OVA conjugates

Aldehyde-modified HA (HA-ALD) was synthesized as described elsewhere.^[53] OVA (5 mg mL⁻¹) and HA-ALD with an aldehyde content of 15 mol% was dissolved in sodium acetate buffer (pH 5.0), and HA-OVA conjugate was formed by the coupling reaction between ALD of HA-ALD and the N-terminal amine group of OVA. After conjugation, 5 molar excess of ethyl carbazate was added and stirred for 24 h to block the residual aldehyde group in HA-OVA conjugates. Sodium cyanoborohydride with 5 molar excess of HA repeating unit was added for the reduction of hydrazine bonds at room temperature for 24 h. The resulting HA-OVA conjugate solution was filtered with a 0.45 µm syringe filter and purified using a centrifugal filter (MWCO of 50 kDa, Millipore, Darmstadt, Germany) to remove unreacted OVA and other chemicals. For bioimaging and FACS analysis, HA, OVA, and HA-OVA conjugate were labeled with Lissamine rhodamine B sulfonyl chloride (RhoB) or fluorescein isothiocyanate (FITC). RhoB was dissolved in dimethylformamide at a concentration of 10 mg mL⁻¹, and 10 molar excess of RhoB was added to the solutions of amine-modified HA, OVA and HA-OVA conjugate dissolved in sodium carbonate buffer (pH 9.0), respectively. The reaction mixture stirred at room temperature for 2 h in the dark and purified using PD 10 desalting columns. The degree of labeling modification was assessed by measuring the absorbance at 280 nm and 540 nm. FITC was labelled using the same method as RhoB, but the degree of labeling modification was assessed by measuring the absorbance at 280 nm and 494 nm.

Characterization of HA-OVA conjugates

The synthesized HA-OVA conjugates were characterized by GPC analysis by comparing the retention time before and after conjugation of HA and OVA. The bio-conjugation efficiency of OVA was calculated by analyzing the GPC peak area of unreacted OVA before purification. GPC analysis was performed using the following systems: Waters 717 plus autosampler, Waters 1525 binary HPLC pump, Waters 2487 dual λ absorbance detector, Ultrahydrogel™ 1000 connected with Ultrahydrogel™ 500 column. The mobile phase was PBS at pH 7.4 and the flow rate was 0.5 mL min⁻¹. The detection wavelength was 280 nm. The secondary structure of HA-OVA conjugate was analyzed by CD spectroscopy. CD spectra of HA-ALD, OVA, and HA-OVA conjugates, and the mixture of HA-ALD and OVA dissolved in PBS were obtained with a spectrum-polarimeter (J-715, JASCO, Easton, MD) at a step size of 0.5 nm. The microenvironment around Trp residues in OVA, HA-OVA conjugate, and the mixture of HA-ALD and OVA dissolved in PBS was assessed by fluorescence spectroscopy using a spectrofluorometer (Cary Eclipse Fluorescence Spectrophotometer, Agilent Technologies, Santa Clara, CA) with excitation at 280 nm. The immunological affinity of OVA and HA-OVA conjugates to anti-OVA antibody was assessed by OVA ELISA based on the absorbance at 450 nm with a microplate reader (SpectraFluor

Plus, TECAN, Mannedorf, Switzerland). The serum stability of OVA and HA-OVA was evaluated by ELISA after incubation in human serum at a concentration of 0.5 mg mL⁻¹ and 37 °C for up to 4 days.

In vitro immunization of HA-OVA conjugates

To assess the maturation of DCs, treated JAWS II cells were stained with MHC-class-II antibody-Alexa 488, CD11c antibody-Alexa 647 conjugates, and DAPI for 1 h, and washed with PBS. Cell morphologies were observed with a confocal microscope (FV1000, Olympus America Inc., Tokyo, Japan). The matured DCs were counted from microscope images. In addition, *in vitro* immunization was assessed by measuring the amount of cytokine and chemokine from 10⁵ JAWS II cells. HA, OVA and HA-OVA conjugates in 500 µl of α-MEM containing 2 vol% FBS with ribonucleosides, deoxyribonucleosides, 4 mM L-glutamine, 1 mM sodium pyruvate, and 5 ng mL⁻¹ murine GM-CSF were added to the cells in culture plates and incubated for 12 h, followed by the addition of 500 µl culture medium. At 1 and 2 days after treatment, respectively, samples of the incubation medium (100 µl) were collected and the whole medium was replaced with 100 µl of fresh 2% FBS containing medium. The amount of cytokine and chemokine in the samples was measured by using ELISA.

Mice

8-week-old wild-type BALB/c mice for investigating immune response, wild-type C57BL/6 mice for investigating skin penetration through imaging, and MHC class II⁺ eGFP⁺ transgenic mice in C57BL/6 background^[54] bred in pathogen-free facilities at Harvard Medical School (HMS) and Pohang University of Science and Technology (POSTECH) were used in this study. All live animal experiments were approved by the HMS Institutional Animal Care and Use Committee (#05052) and the Ethics Committee of POSTECH.

Fluorescence imaging of transdermal delivery

PBS, OVA-RhoB, HA-RhoB, or HA-OVA-RhoB conjugates containing the same amount of OVA (50 µg) and HA (100 µg) was topically applied on the hair-removed mouse skin. An adhesive patch was attached onto the applied area to minimize drying. The retrieved skin tissues after 4 h were fixed in 4% paraformaldehyde solution, embedded into optimal cutting temperature compound (OCT) at -70 °C, and cut into 5 µm-thick sections. The sections were fixed with cold acetone at -20 °C and washed with distilled water to remove the residual OCT resins on the slide. Histological tissue sections were imaged by using a home-built confocal microscope. For intravital microscopy, the hair in the dried skin on the back was removed carefully using an electrical animal clipper, which maintain the barrier function of the stratum corneum. Depilating agents were not used to exclude any potential effects on DCs in the skin.^[55] Anesthetized MHC class II⁺ eGFP⁺ mice were placed on a temperature-controlled stage. OVA-RhoB or HA-OVA-RhoB conjugates was applied to the shaved and intact skin. *In vivo* imaging was performed with a custom-built, video-rate, two-photon microscope using a Ti:Sapphire laser (Mai-Tai DeepSee, Spectra-Physics, Santa Clara, CA) and a water immersion objective lens (20×, 0.9 NA), as previously described.^[56] The excitation wavelength was set to 810 nm, and the optical power at the sample was approximately 150 mW. The image analysis and the generation of time-lapse image sequences were performed using Image J and custom software.

LN analysis

Histological analysis of dissected cervical LNs was carried out with a home-built two-photon microscope 2 days post-topical administration at the back neck skin of MHC class II⁺ eGFP⁺ mice. For further flow cytometric analysis, 0.5 mg of FITC-conjugated HA-OVA conjugates were applied to the abdominal flank skin, and draining inguinal LNs were collected 2, 4, and 6 days. The cells from the tissues were stained with allophycocyanin-conjugated anti-CD11c, Pacific Blue-conjugated anti-IA/IE, phycoerythrin-cyanin7-conjugated anti-CD8 α , and phycoerythrin-conjugated anti-CD103 (all from eBioscience, San Diego, CA) and analyzed by flow cytometry using BD FACSCanto™ II (BD Bioscience, San Diego, CA) and FlowJo program (FlowJo, LLC, Ashland, OR).

Laser adjuvant

A commercial battery-powered hand-held laser device (PaloVia Skin Renewing System, Palomar Medical Technologies), which has been originally approved and marketed for home skin care,^[57] was used for laser adjuvant. Upon each trigger, the device emits a 6 × 9 array of laser beams at a center wavelength 1410 (+/- 20) nm for pulse duration of 10 ms. The pulse energy was set to 0.2 mJ per pulse. The pulse energy, duration, wavelength, and beam focal depth were optimized so that the non-ablative beam affects the dermis while leaving the skin surface intact. After the laser head was made in contact to the hair-shaved skin, the device was triggered three times depositing about 32.4 mJ of optical energy to a 9 mm by 13 mm area. Its adjuvant effects on APCs is described in detail elsewhere [21, 22].

In vivo immunization & sample collection

In vivo immunization experiments were carried out using BALB/c mice with a mean body weight of 20 g. HA-OVA conjugates (20 μ g of OVA) were administered using a needle intramuscularly. Topical transdermal administration was conducted with HA-OVA conjugate containing 20, 200, or 500 μ g of OVA. The skin patch covering the applied agents was removed after 48 hours. For comparison, free OVA at various doses (20, 200 and 500 μ g) were administered using the same protocol. Laser-adjuvant was given to the skin before the topical treatment of HA-OVA conjugates. Blood samples were harvested 4 weeks post-administration of OVA and HA-OVA conjugates. In addition, to investigate time dependence of immune responses, blood samples were collected 2, 4 and 8 weeks after administration, respectively. In addition, to estimate mucosal immunity, BAL fluid also collected as described elsewhere.^[15, 58] To investigate recall immune response, 50 μ g of OVA was injected into the mice 8 weeks after topical application of OVA and HA-OVA conjugates (500 μ g of OVA). Four days after the immune challenge, blood samples were harvested and analyzed for humoral immune responses.

Anti-OVA IgG & IgA analysis

The immunization of HA-OVA conjugates was evaluated by anti-OVA IgG & IgA antibody ELISA. OVA solution at a concentration of 10 μ g mL⁻¹ in sodium carbonate buffer was incubated in 96-well plate for 1 h at room temperature. After washing thrice with TTBS, the wells were incubated with 1% skim milk. After washing with TTBS, anti-mouse OVA antibody standard solutions and blood samples diluted in PBS were added to the well and

incubated at room temperature for 1 h. After washing with TTBS, goat anti-mouse IgG antibody-HRP conjugate solution at a concentration of $0.3 \mu\text{g mL}^{-1}$ in PBS was added to the well and incubated at room temperature for 1 h. Finally, after washing with TTBS, the wells were incubated with TMB solution followed by 2 N H_2SO_4 stop solution. The absorbance was measured at 450 nm with a microplate reader. ELISA was performed twice with four replicates. In case of IgA, we carried out same procedure using anti-mouse IgA antibody-HRP conjugates.

Porcine experiment

Porcine neck skin tissues ($10 \times 10 \text{ cm}^2$ each) were extracted from 3-month-old pigs immediately after post mortem at Knight Laboratory in the Department of Surgery at MGH, as approved by the MGH Subcommittee on Research Animal Care (#2014N000049). After hair-removal of the porcine skin using animal clipper,^[42] OVA-RhoB or HA-OVA-RhoB (250 μg of OVA each) was topically applied to the 2-cm-wide central regions of the tissues. At different time points (2 to 6 h) after administration, cross-sectional tissue sections were obtained and analyzed by two-photon microscopy.

Statistical analysis

Data are expressed as means \pm standard deviation from several animals in a group in a few separate experiments. Statistical analysis was carried out with the two-way analysis of variance (ANOVA) test using SigmaPlot10.0 (Systat Software, Inc., San Jose, CA). P values less than 0.05 were considered statistically significant.

Supplementary Material

Refer to Web version on PubMed Central for supplementary material.

Acknowledgments

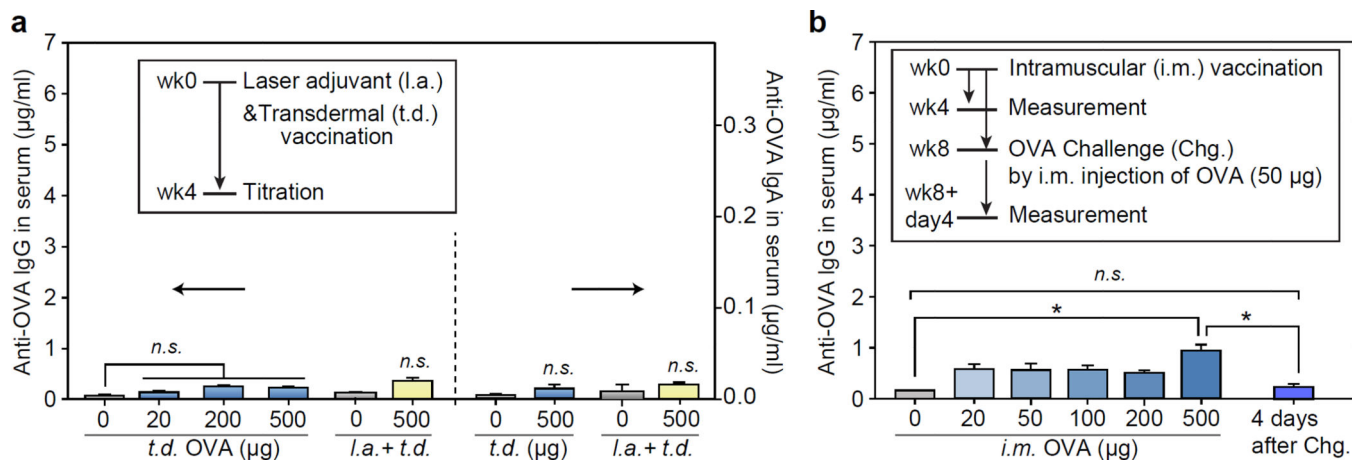
We thank Dr. Myunghwan Choi and Dr. Jie Zhao for help in intravital imaging and histological analysis, Dr. Mark Randolph for providing access to experimental pigs, Dr. Jeeseo An for help in interpretation of histology, and Dr. Ji Wang and Prof. Mei Wu for discussion. This study was supported by Mid-career Researcher Program through the National Research Foundation of Korea grant funded by the Ministry of Education, Science and Technology (No. 2012R1A2A2A06045773) and in part by National Institutes of Health (P41-EB015903, R01-CA192878, P01-HL120839).

References

1. Plotkin SA. Nat Med. 2005; 11:S5. [PubMed: 15812490]
2. Moon JJ, Suh H, Bershteyn A, Stephan MT, Liu H, Huang B, Sohail M, Luo S, Ho Um S, Khant H, Goodwin JT, Ramos J, Chiu W, Irvine DJ. Nat Mater. 2011; 10:243. [PubMed: 21336265]
3. Bachmann MF, Jennings GT. Nature reviews. Immunology. 2010; 10:787.
4. Kenney RT, Frech SA, Muenz LR, Villar CP, Glenn GM. The New England journal of medicine. 2004; 351:2295. [PubMed: 15525714]
5. Chen D, Endres RL, Erickson CA, Weis KF, McGregor MW, Kawaoka Y, Payne LG. Nat Med. 2000; 6:1187. [PubMed: 11017153]
6. Polat BE, Hart D, Langer R, Blankschtein D. Journal of controlled release : official journal of the Controlled Release Society. 2011; 152:330. [PubMed: 21238514]
7. Hirao LA, Wu L, Khan AS, Satishchandran A, Draghia-Akli R, Weiner DB. Vaccine. 2008; 26:440. [PubMed: 18082294]

7. Pissuwan D, Nose K, Kurihara R, Kaneko K, Tahara Y, Kamiya N, Goto M, Katayama Y, Niidome T. *Small*. 2011; 7:215. [PubMed: 21213384]
8. Torchilin VP. *Nat Rev Drug Discov*. 2005; 4:145. [PubMed: 15688077]
9. Su, X.; Kim, B-S.; Kim, SR.; Hammond, PT.; Irvine, DJ. *ACS nano*. Vol. 3. American Chemical Society; 2009. p. 3719
10. Huang Y, Park YS, Moon C, David AE, Chung HS, Yang VC. *Angew Chem Int Ed Engl*. 2010; 49:2724. [PubMed: 20232417]
11. Rappuoli R, Mandl CW, Black S, De Gregorio E. *Nature reviews. Immunology*. 2011; 11:865.
12. Rechtsteiner G, Warger T, Osterloh P, Schild H, Radsak MP. *The Journal of Immunology*. 2005; 174:2476. [PubMed: 15728450]
13. Glenn GM, Taylor DN, Li X, Frankel S, Montemarano A, Alving CR. *Nat Med*. 2000; 6:1403. [PubMed: 11100128]
14. Petrovsky N, Aguilar JC. *Immunol Cell Biol*. 2004; 82:488. [PubMed: 15479434]
15. Sullivan SP, Koutsonanos DG, Del Pilar Martin M, Lee JW, Zarnitsyn V, Choi SO, Murthy N, Compans RW, Skountzou I, Prausnitz MR. *Nat Med*. 2010; 16:915. [PubMed: 20639891]
16. DeMuth PC, Min Y, Huang B, Kramer JA, Miller AD, Barouch DH, Hammond PT, Irvine DJ. *Nat Mater*. 2013; 12:367. [PubMed: 23353628] Bachy V, Hervouet C, Becker PD, Chorro L, Carlin LM, Herath S, Papagatsias T, Barbaroux JB, Oh SJ, Benlahrech A, Athanasopoulos T, Dickson G, Patterson S, Kwon SY, Geissmann F, Klavinskis LS. *Proceedings of the National Academy of Sciences of the United States of America*. 2013; 110:3041. [PubMed: 23386724]
17. Kupper TS, Fuhlbrigge RC. *Nature reviews. Immunology*. 2004; 4:211.
18. Chen X, Kim P, Farinelli B, Doukas A, Yun S-H, Gelfand JA, Anderson RR, Wu MX. *PLoS ONE*. 2010; 5:e13776. [PubMed: 21048884]
19. Chen X, Shah D, Kosiratna G, Manstein D, Anderson RR, Wu MX. *Journal of controlled release : official journal of the Controlled Release Society*. 2012; 159:43. [PubMed: 22261281]
20. Kashiwagi S, Yuan J, Forbes B, Hibert ML, Lee ELQ, Whicher L, Goudie C, Yang Y, Chen T, Edelblute B, Collette B, Edington L, Trussler J, Nezivar J, Leblanc P, Bronson R, Tsukada K, Suematsu M, Dover J, Brauns T, Gelfand J, Poznansky MC. *PloS one*. 2013; 8:e82899. [PubMed: 24349390]
21. Wang J, Li B, Wu MX. *Proceedings of the National Academy of Sciences*. 2015; 112:5005.
22. Wang J, Shah D, Chen X, Anderson RR, Wu MX. *Nat Commun*. 2014:5.
23. Brown TJ, Alcorn D, Fraser JR. *The Journal of investigative dermatology*. 1999; 113:740. [PubMed: 10571728]
24. Brown MB, Jones SA. *Journal of the European Academy of Dermatology and Venereology : JEADV*. 2005; 19:308. [PubMed: 15857456]
25. Tammi R, Saamanen AM, Maibach HI, Tammi M. *The Journal of investigative dermatology*. 1991; 97:126. [PubMed: 2056182]
26. Witting M, Boreham A, Brodewolf R, Vavrova K, Alexiev U, Friess W, Hedtrich S. *Mol Pharm*. 2015; 12:1391. [PubMed: 25871518]
27. Yang JA, Kim ES, Kwon JH, Kim H, Shin JH, Yun SH, Choi KY, Hahn SK. *Biomaterials*. 2012; 33:5947. [PubMed: 22632765]
28. Singh M, Briones M, O'Hagan DT. *Journal of Controlled Release*. 2001; 70:267. [PubMed: 11182197]
29. Jung HS, Kong WH, Sung DK, Lee M-Y, Beack SE, Keum DH, Kim KS, Yun SH, Hahn SK. *ACS nano*. 2014; 8:260. [PubMed: 24383990]
30. Termeer C, Benedix F, Sleeman J, Fieber C, Voith U, Ahrens T, Miyake K, Freudenberg M, Galanos C, Simon JC. *The Journal of experimental medicine*. 2002; 195:99. [PubMed: 11781369]
31. Kono H, Rock KL. *Nature reviews. Immunology*. 2008; 8:279. Jiang D, Liang J, Fan J, Yu S, Chen S, Luo Y, Prestwich GD, Mascarenhas MM, Garg HG, Quinn DA, Homer RJ, Goldstein DR, Bucala R, Lee PJ, Medzhitov R, Noble PW. *Nat Med*. 2005; 11:1173. [PubMed: 16244651]
32. Leyden J, Stephens TJ, Herndon JH Jr. *Journal of the American Academy of Dermatology*. 2012; 67:975. [PubMed: 22386051]
33. Klinman DM, Barnhart KM, Conover J. *Vaccine*. 1999; 17:19. [PubMed: 10078603]

34. Slutter B, Soema PC, Ding Z, Verheul R, Hennink W, Jiskoot W. *Journal of controlled release : official journal of the Controlled Release Society*. 2010; 143:207. [PubMed: 20074597]
35. Kinster O, Molineux G, Treuheit M, Ladd D, Gegg C. *Advanced Drug Delivery Reviews*. 2002; 54:477. [PubMed: 12052710] Tao L, Mantovani G, Lecolley F, Haddleton DM. *Journal of the American Chemical Society*. 2004; 126:13220. [PubMed: 15479065]
36. Eiser E, Miles CS, Geerts N, Verschuren P, MacPhee CE. *Soft Matter*. 2009; 5:2725.
37. Burger K, Illes J, Gyurcsik B, Gazdag M, Forrai E, Dekany I, Mihalyfi K. *Carbohydrate research*. 2001; 332:197. [PubMed: 11434378]
38. Leggatt GR, Dunn LA, De kluyver RL, Stewart T, Frazer IH. *Immunol Cell Biol*. 2002; 80:415. [PubMed: 12225377]
39. Do Y, Nagarkatti PS, Nagarkatti MP. *Journal of Immunotherapy*. 2004; 27:1. [PubMed: 14676629]
40. Villadangos JA, Cardoso Ma, Steptoe RJ, van Berkel D, Pooley J, Carbone FR, Shortman K. *Immunity*. 2001; 14:739. [PubMed: 11420044]
41. Avci FY, Li X, Tsuji M, Kasper DL. *Nat Med*. 2011; 17:1602. [PubMed: 22101769]
42. Karande P, Jain A, Mitragotri S. *Nat Biotech*. 2004; 22:192.
43. Fan H, Lin Q, Morrissey GR, Khavari PA. *Nature biotechnology*. 1999; 17:870.
44. Henri S, Poulin LF, Tamoutounour S, Ardouin L, Guilliams M, de Bovis B, Devillard E, Viret C, Azukizawa H, Kissenpfennig A, Malissen B. *The Journal of experimental medicine*. 2010; 207:189. [PubMed: 20038600]
45. Bedoui S, Whitney PG, Waithman J, Eidsmo L, Wakim L, Caminschi I, Allan RS, Wojtasiak M, Shortman K, Carbone FR, Brooks AG, Heath WR. *Nature immunology*. 2009; 10:488. [PubMed: 19349986]
46. Wang Y, Marshall KL, Baba Y, Gerling GJ, Lumpkin EA. *PLoS one*. 2013; 8:e67439. [PubMed: 23825661]
47. Muto J, Morioka Y, Yamasaki K, Kim M, Garcia A, Carlin AF, Varki A, Gallo RL. *The Journal of clinical investigation*. 2014; 124:1309. [PubMed: 24487587]
48. Termeer CC, Hennies J, Voith U, Ahrens T, Weiss JM, Prehm P, Simon JC. *J Immunol*. 2000; 165:1863. [PubMed: 10925265]
49. Banga, AK. *Therapeutic Peptides and Proteins: Formulation, Processing, and Delivery Systems*. Boca Raton, FL, USA: CRC Press; 2006.
50. Ishii Y, Nakae T, Sakamoto F, Matsuo K, Matsuo K, Quan Y-S, Kamiyama F, Fujita T, Yamamoto A, Nakagawa S, Okada N. *Journal of Controlled Release*. 2008; 131:113. [PubMed: 18700159]
51. Ives M, Melrose S. *Nursing Forum*. 2010; 45:29. [PubMed: 20137022] Kettwich SC, Sibbitt WL, Brandt JR, Johnson CR, Wong CS, Bankhurst AD. *Journal of Pediatric Oncology Nursing*. 2007; 24:20. [PubMed: 17185398]
52. Hamilton JG. *J Fam Pract*. 1995; 41:169. [PubMed: 7636457]
53. Yang JA, Park K, Jung H, Kim H, Hong SW, Yoon SK, Hahn SK. *Biomaterials*. 2011; 32:8722. [PubMed: 21872329]
54. Boes M, Cerny J, Massol R, Op den Brouw M, Kirchhausen T, Chen J, Ploegh HL. *Nature*. 2002; 418:983. [PubMed: 12198548]
55. Sen D, Forrest L, Kepler TB, Parker I, Cahalan MD. *Proceedings of the National Academy of Sciences of the United States of America*. 2010; 107:8334. [PubMed: 20404167]
56. Choi M, Yun SH. *Optics Express*. 2013; 21:30842. [PubMed: 24514657]
57. Manstein D, Herron GS, Sink RK, Tanner H, Anderson RR. *Lasers in Surgery and Medicine*. 2004; 34:426. [PubMed: 15216537]
58. Bessa J, Jegerlehner A, Hinton HJ, Pumpens P, Saudan P, Schneider P, Bachmann MF. *The Journal of Immunology*. 2009; 183:3788. [PubMed: 19710454]

**Figure 1.**

(a) Induction of OVA-specific humoral and mucosal immune response 4 weeks after transdermal (*t.d.*) administration (blue), and laser-adjuvant (*l.a.*) transdermal administration (yellow) of OVA (mean \pm SD, $n = 4$); n.s., $P > 0.05$. (b) OVA-specific antibody titers measured at 4 weeks after intramuscular (*i.m.*) injection of OVA (500 µg) and 4 days after OVA challenge test (mean \pm SD, $n = 4$); *, $P < 0.05$.

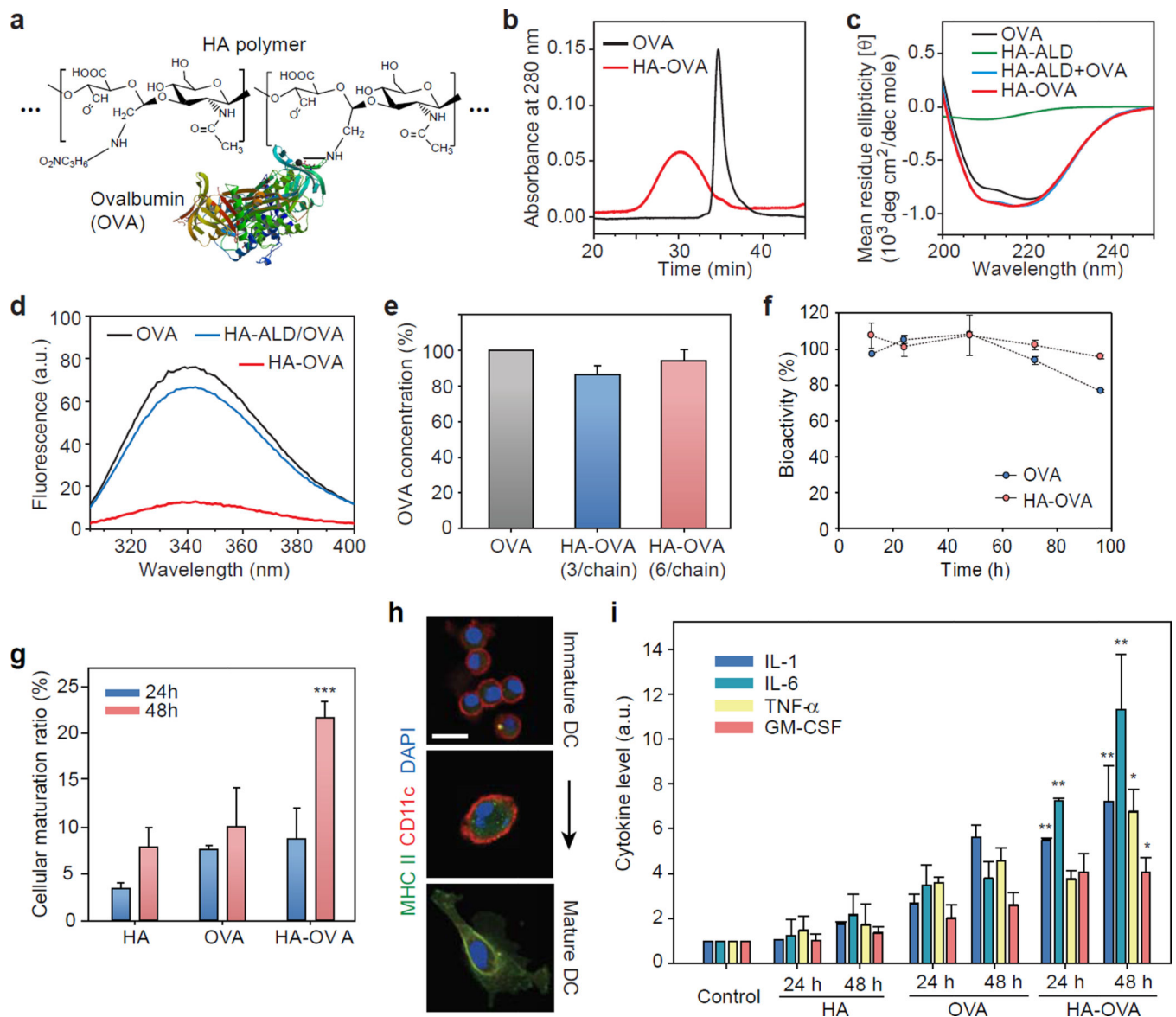


Figure 2. Characterization of HA-OVA conjugates. (a) The chemical structure of HA-OVA conjugates. (b) Gel permeation chromatograms of OVA (black) and HA-OVA conjugate (red). (c) Circular dichroism spectra of OVA (black), HA-ALD (green), the mixture of OVA and HA-ALD (blue), and HA-OVA conjugate (red). (d) Fluorescence emission spectra of OVA (black), the mixture of OVA and HA-ALD (blue), and HA-OVA conjugate (red). (e) The ratio of bioactive OVA in HA-OVA. Error bars, s.d. (f) *In vitro* stability of OVA and HA-OVA conjugates in human serum. (g) The ratios of matured JAWS II cells 24 and 48 h after treatment with OVA, HA and HA-OVA conjugate, respectively (mean \pm SD, $n = 5$). **, $P < 0.01$, w.r.t. HA-OVA. (h) Confocal fluorescence images of immature and matured DCs stained with anti-MHCII-Alexa 488 (green), anti-CD11c-Alexa 647 (red), and nuclear-dye Hoechst (blue). (i) Cytokine levels measured by ELISA from JAWS II cells treated with

OVA, HA and HA-OVA conjugates for 24 h and 48 h (mean \pm SD, n = 5). *, $P < 0.05$; **, $P < 0.01$, HA-OVA vs. other groups. Scale bars, 10 μm in (h).

Author Manuscript

Author Manuscript

Author Manuscript

Author Manuscript

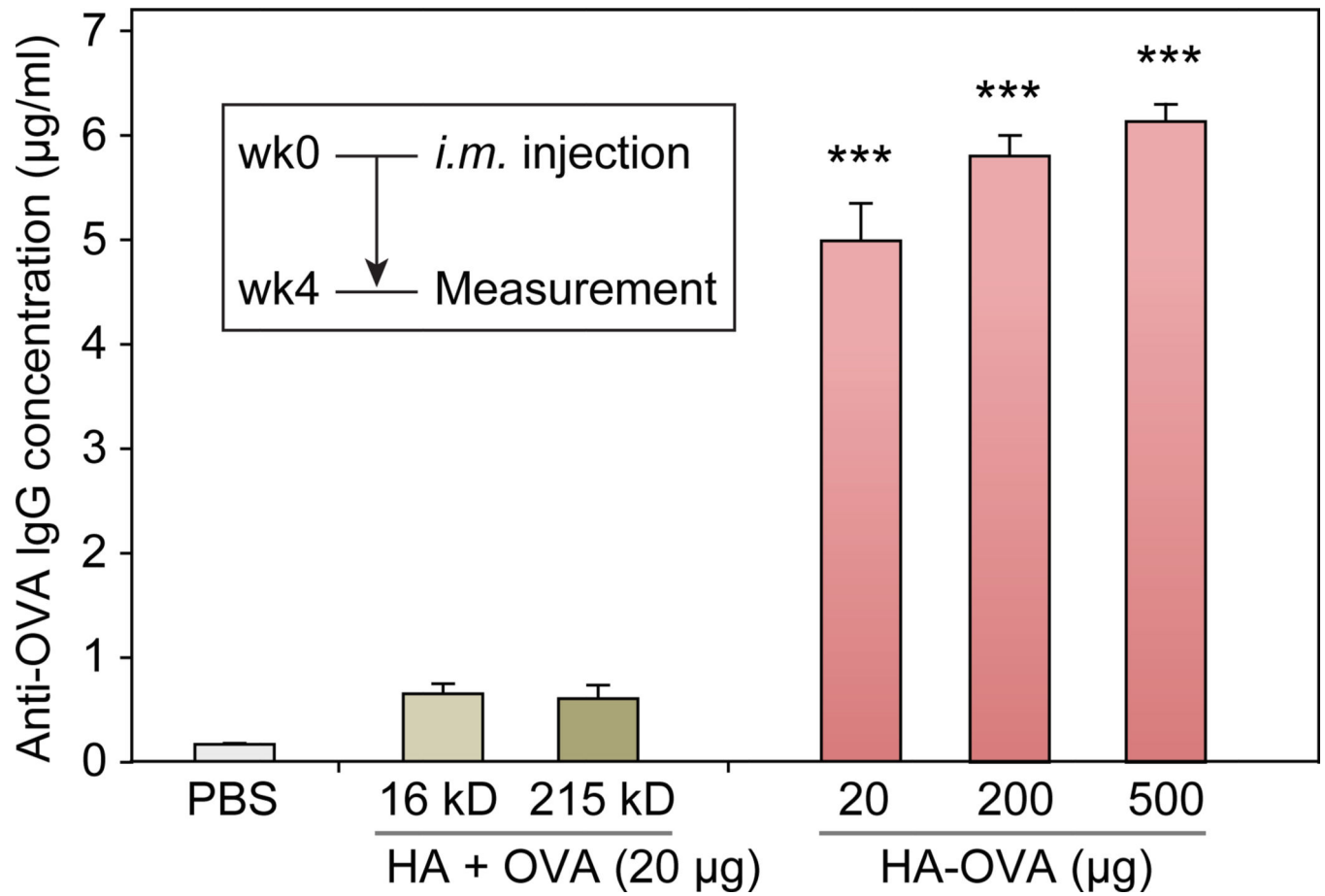


Figure 3. OVA-specific IgG antibody titers measured by ELISA 4 weeks after intramuscular (*i.m.*) injection of different agents (mean \pm SD, $n=4$). ***, $P < 0.001$.

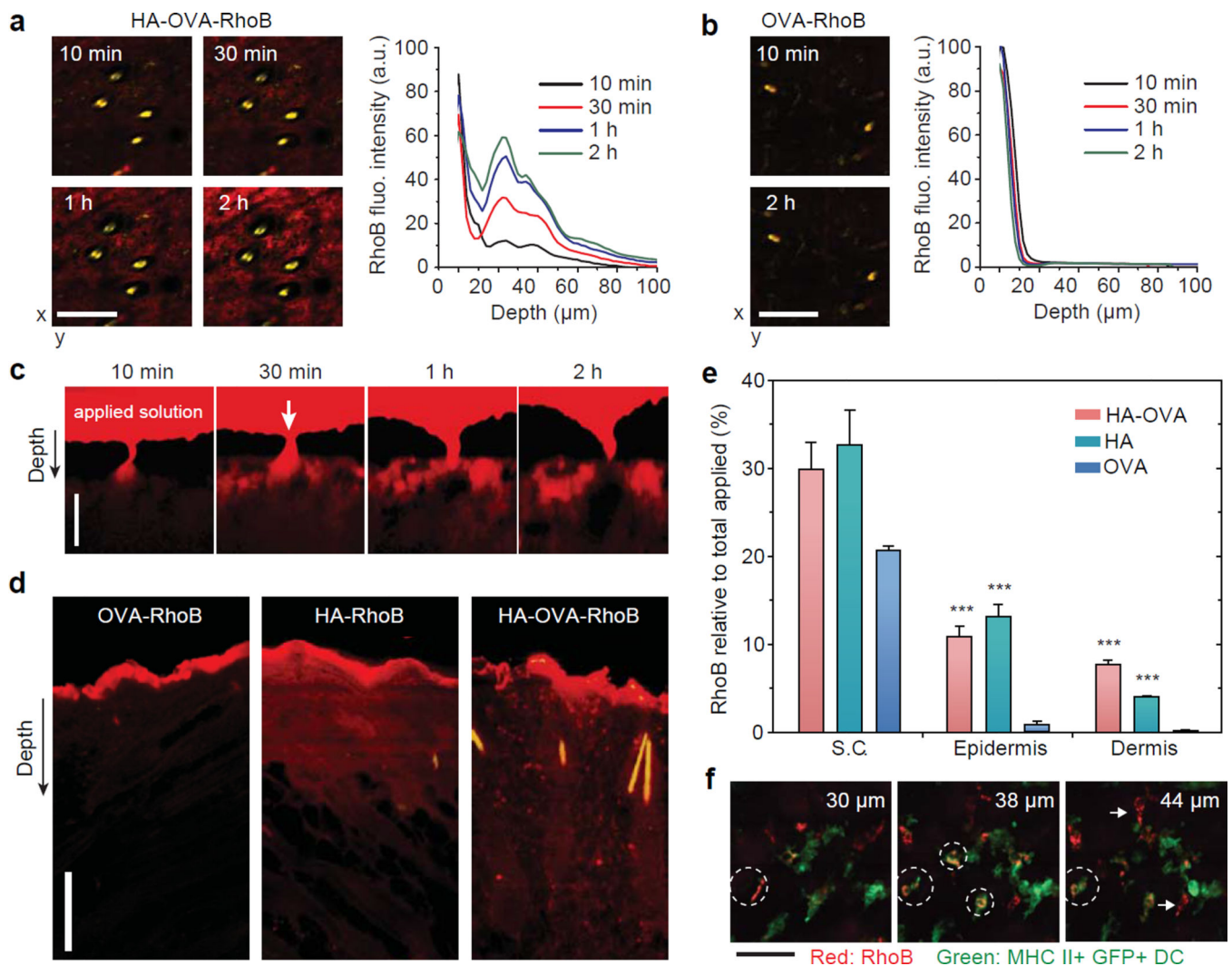
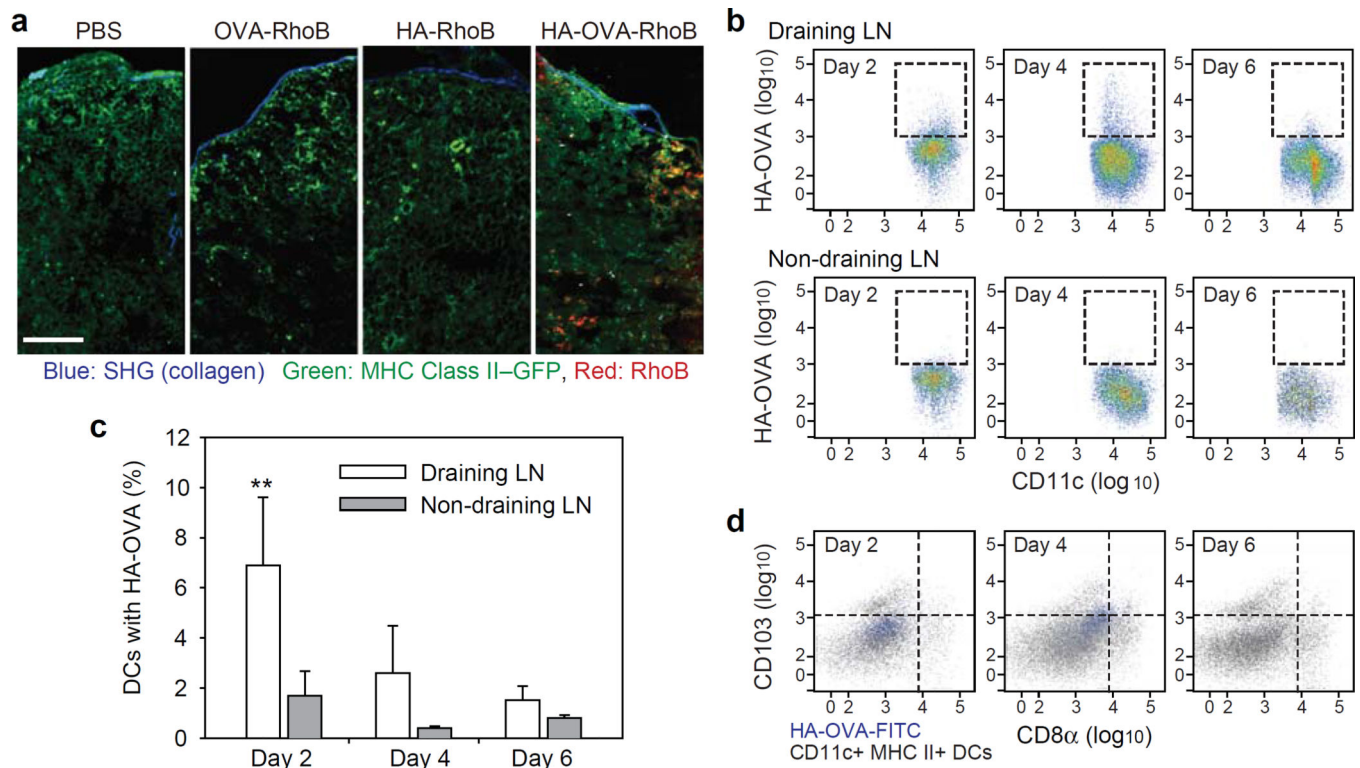


Figure 4. Two-photon excited fluorescence *en face* images and depth profiles of the murine skin in the dermis *in vivo* post topical administration of (a) HA-OVA-RhoB and (b) OVA-RhoB conjugates. (c) *In vivo* time-lapse images of HA-OVA-RhoB conjugate after topical administration. On top of the tissue, a reservoir of the applied agent in solution (red) is seen. Arrow indicates the position of a wrinkle line. (d) Confocal fluorescence images of histological sections harvested 4 h after the topical application of OVA-RhoB, HA-RhoB, and HA-OVA-RhoB conjugates, respectively. (e) Quantification of RhoB fluorescence intensity in the stratum corneum (S.C.), epidermis, and dermis layers. One hundred % represents the total amount applied to the skin including that remaining in solution (see the text) (mean \pm SD, n = 7). ***, P-value < 0.001 w.r.t. OVA-RhoB. (f) Z-sectioned confocal images of HA-OVA-RhoB conjugate (red) and MHC class II+ eGFP+ DCs (green) in the dermis *in vivo*. White dashed circles mark dermal DCs associated with HA-OVA-RhoB conjugate, and white arrows indicate the interaction of HA-OVA-RhoB conjugate presumably with other HA-receptor expressing cells, such as fibroblasts. Scale bars, 100 μm in (a, b), 25 μm in (c, d) and 50 μm in (f).

**Figure 5.**

(a) Two-photon microscopic image of histological sections of skin-draining LNs 2 days after treatment with PBS, OVA-RhoB, HA-RhoB, and HA-OVA-RhoB conjugates, respectively, on the back skin of mice. Scale bar, 100 μ m. (b) Cytometry plots of HA-OVA-FITC conjugate containing CD11c⁺ DCs in skin draining LNs (Top) and non-draining LNs (Bottom), at 2, 4 and 6 days post topical application on abdominal flank. (c) The ratio of CD11⁺ DCs containing HA-OVA-FITC conjugate determined from the cytometry results (mean \pm SD, n = 5). **, $P < 0.01$, Draining LN vs. Non-draining LN. (d) Cytometry analysis for the expression of CD8 α and CD103 of the cells associated with HA-OVA-FITC conjugate or CD11c⁺ MHC II⁺, at 2, 4, and 6 days in draining inguinal LNs.

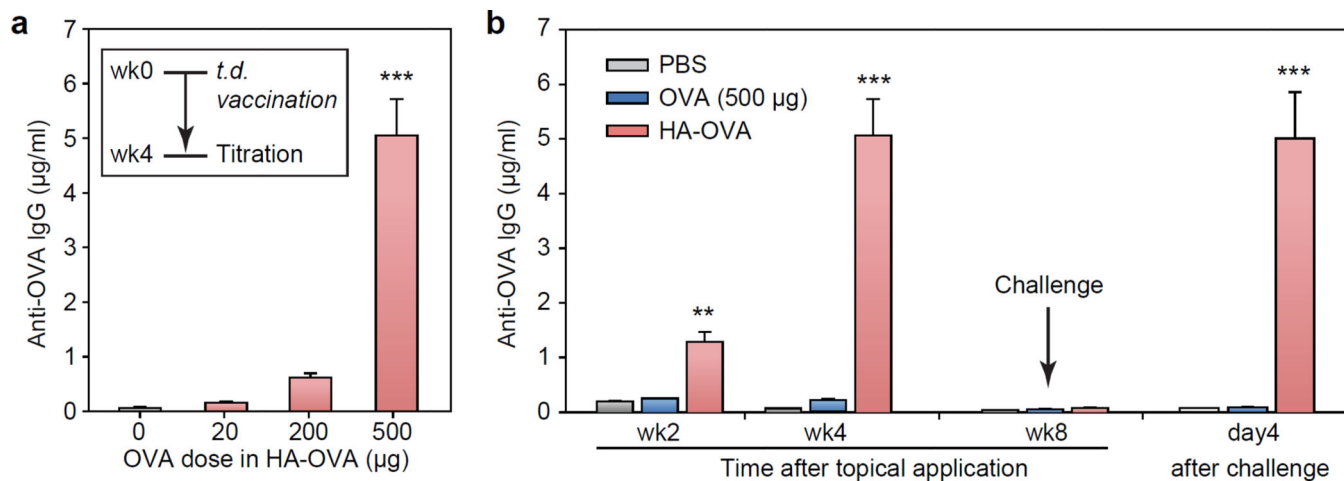


Figure 6.

(a) Induction of OVA-specific humoral immune response 4 weeks after transdermal (*t.d.*) administration of HA-OVA (mean \pm SD, $n = 4$). ***, $P < 0.001$, HA-OVA (500 μg of OVA) vs. HA-OVA with other OVA doses. (b) OVA-specific antibody titers measured at 2, 4 and 8 weeks after transdermal immunization with HA-OVA conjugate (500 μg of OVA) (mean \pm SD, $n = 4$) and 4 days after OVA challenge test. **, $P < 0.01$; ***, $P < 0.001$, HA-OVA vs. OVA.

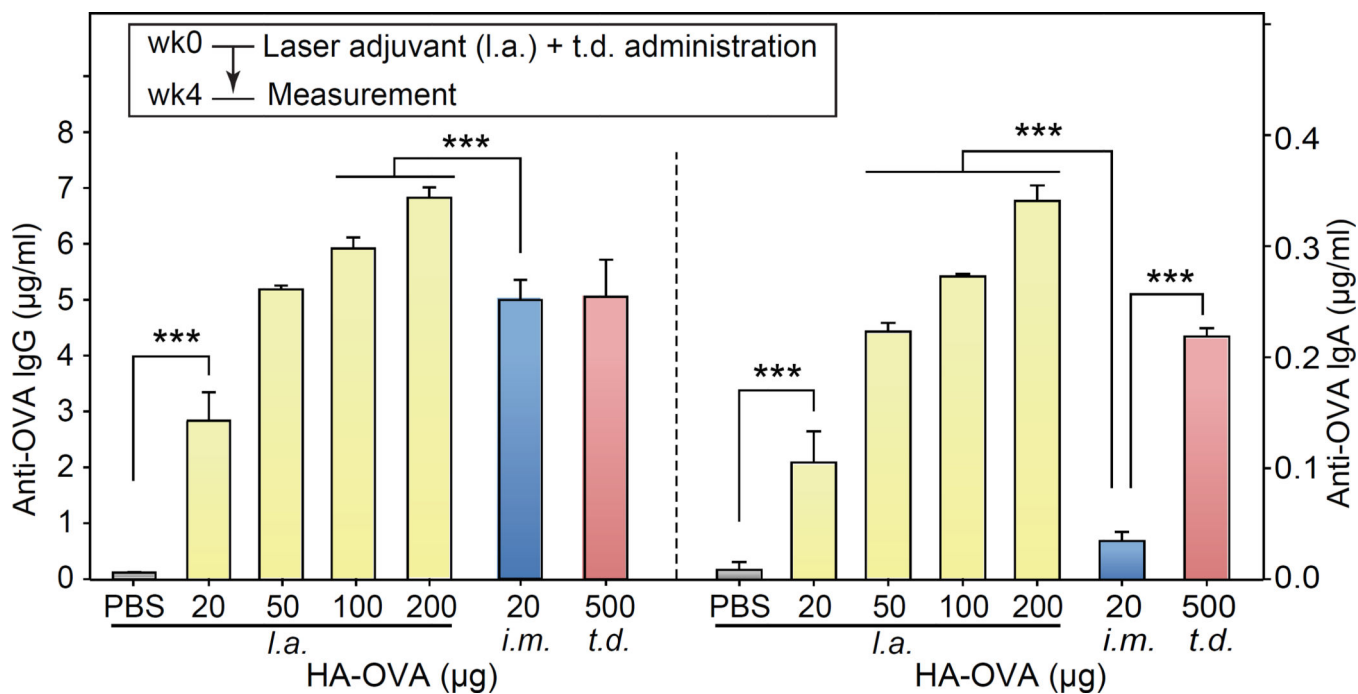


Figure 7. Concentration of OVA-specific IgG (left panel) and IgA (right panel) at 4 weeks after laser adjuvant (l.a.) and topical application of HA-OVA conjugates with various doses (mean \pm SD, $n = 4$), in comparison to intramuscular (i.m.) injection and transdermal (t.d.) application without laser adjuvants. ***, $P < 0.001$.

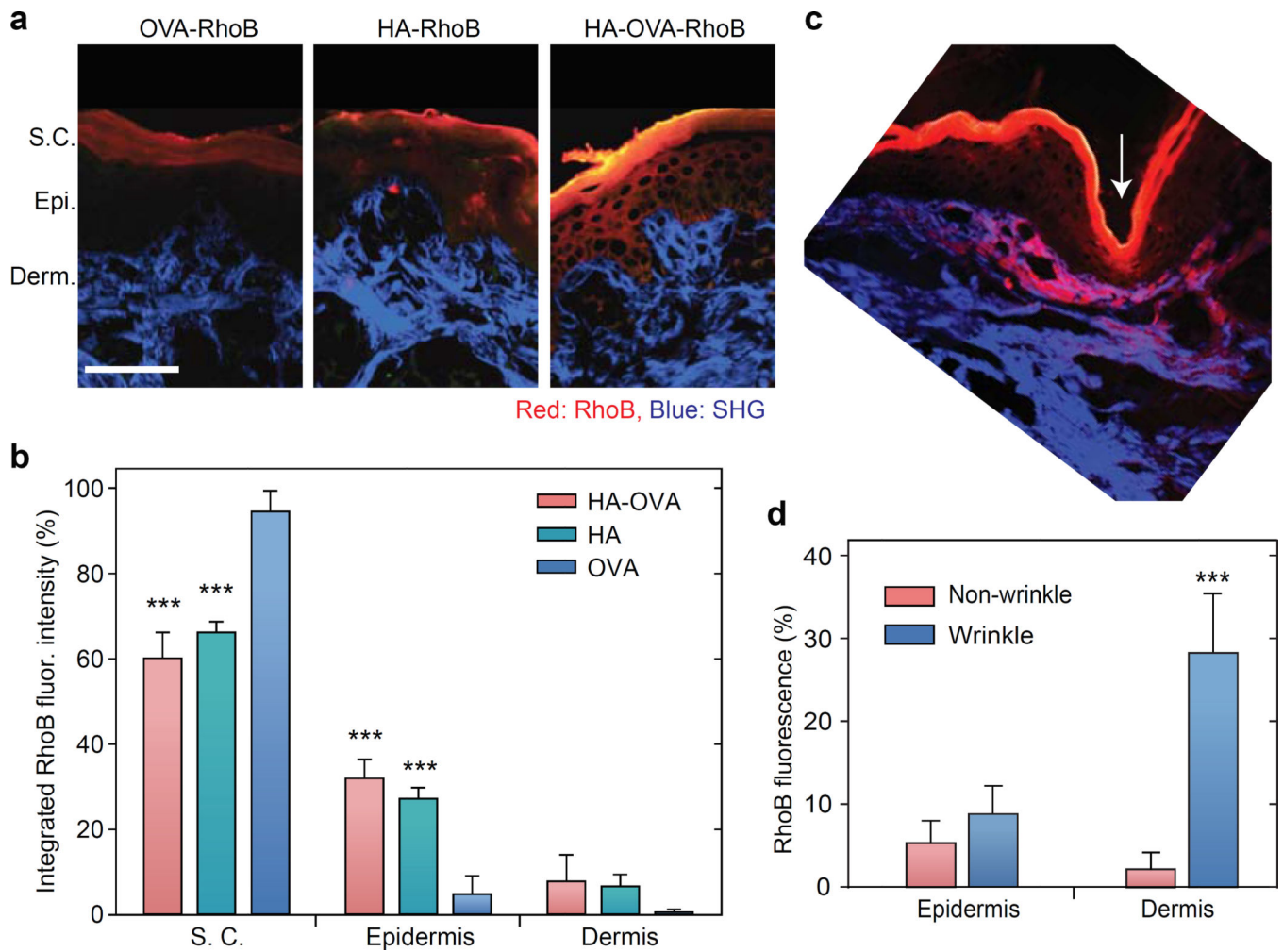


Figure 8.

(a) Two-photon microscope images of histological sections of porcine skins, 6 h after topical application of OVA-RhoB, HA-RhoB and HA-OVA-RhoB conjugates, respectively. Red, RhoB fluorescence; blue, SHG from collagen fibers. S.C., stratum corneum; E., epidermis (E.); D., dermis. Scale bar, 250 μ m. (b) Quantification of RhoB fluorescence intensity ratio integrated over stratum corneum, epidermis, and dermis, respectively, in the porcine skins (mean \pm SD, $n = 7$). ***, $P < 0.001$, w.r.t. OVA-RhoB. (c) Two-photon image of histological section of porcine skin around wrinkle (white arrow) 2h after topical application of HA-OVA-RhoB conjugate. (d) Integrated RhoB fluorescence intensity over epidermis and dermis near wrinkles (white arrow in c) vs. non-wrinkle regions (mean \pm SD, $n = 7$). ***, $P < 0.001$.

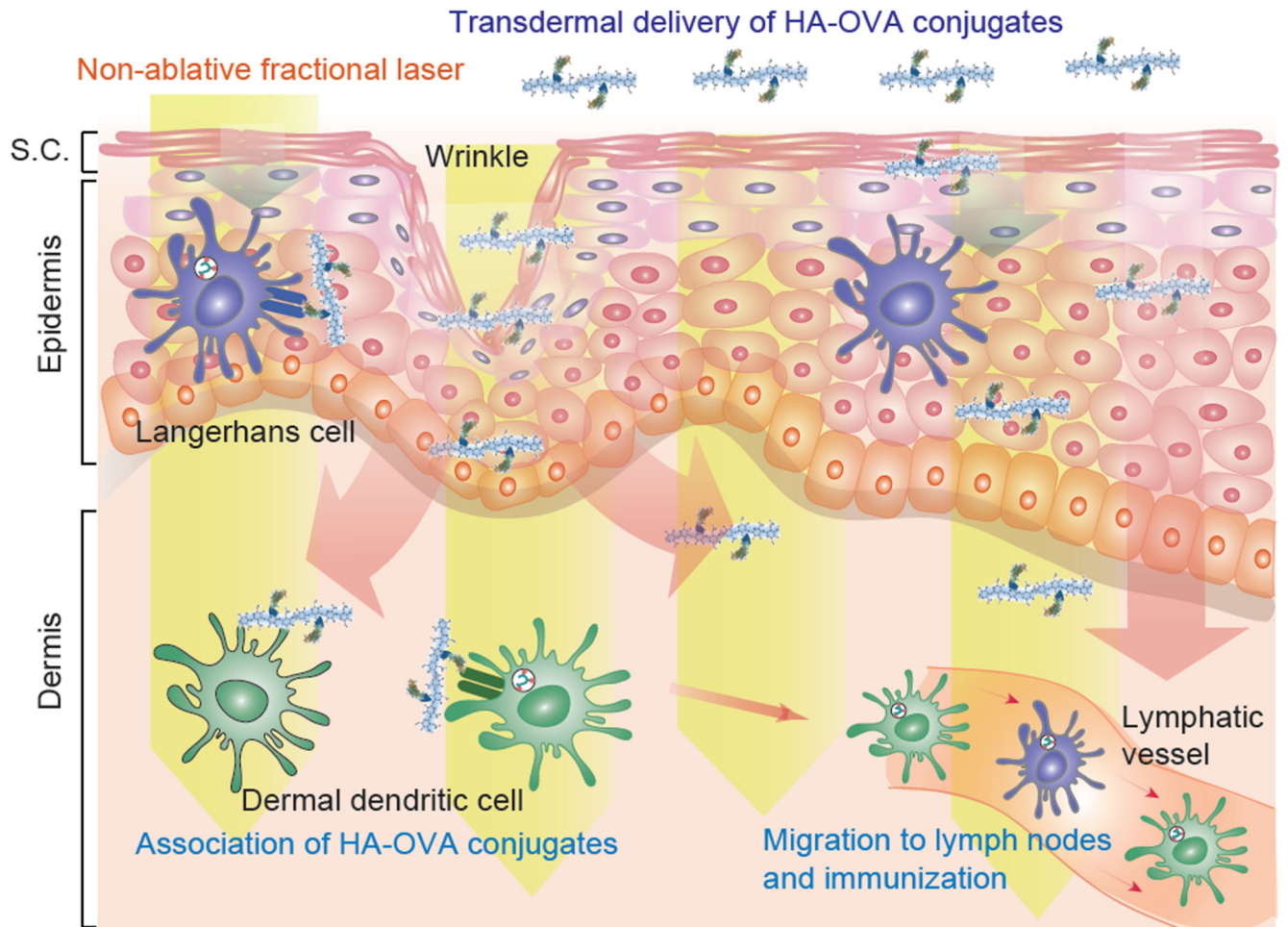


Figure 9. Schematic representation of transdermal immunization by HA-OVA conjugates with laser adjuvant. Topically applied HA-OVA conjugates penetrate into the skin through skin barriers and diffuse throughout the skin. Non-ablative fractional laser adjuvant enhances immune response at the dermis layer. Activated dendritic cells (DCs) migrate to draining lymph nodes and induce immunity.